# Spin−Spin Interactions in the Oxides $A_3M'MO_6$ (M = Rh, Ir; A = Ca, Sr; M′ = Alkaline Earth, Zn, Cd, Na) of the $K_4CdCl_6$ Structure Type Examined by Electronic Structure Calculations

**K.-S. Lee**

Department of Chemistry, The Catholic University of Korea, Puchon, Kyunggi-Do, South Korea 422-743

**H.-J. Koo and M.-H. Whangbo***

Department of Chemistry, North Carolina State University, Raleigh, North Carolina 27695-8204

*Received December 2, 1998*

The oxides $A_3M'MO_6$ (M = Rh, Ir; A = Ca, Sr; M′ = alkaline earth, Zn, Cd) of the $K_4CdCl_6$ structure type consist of isolated $(MO_6)^{8-}$ octahedral anions and exhibit an antiferromagnetic ordering at low temperatures. The spin−spin interactions in these oxides, $Ca_3NaMO_6$ (M = Ir, Ru), and $Sr_3NaRuO_6$ were examined by calculating how strongly the $t_{2g}$-block levels of adjacent $(MO_6)^{(6+n)-}$ ($n$ = 1, 2) anions interact in the presence and absence of the intervening cations $A^{2+}$ and $M'^{n+}$ ($n$ = 1, 2). Our calculations show that the spin−spin interactions in these oxides are three-dimensional, and the superexchange interactions occur mainly through the short intrachain and interchain M−O···O−M linkages. When the $M^{n+}$ cation is very small compared with the $A^{2+}$ cation, the intrachain interaction is substantially stronger than the interchain interaction. The opposite is found when the sizes of the $M^{n+}$ and $A^{2+}$ cations become similar.

## 1. Introduction

The $K_4CdCl_6$-type structure[1] is adopted in a number of oxides $A_3M'MO_6$.[2−17] In these oxides, $MO_6$ (M = Co, Rh, Ir, Pt, Ru) octahedra and $M'O_6$ (M′ = Na, Mg, Ca, Sr, Ba, Ga, Zn, Cd, Co, Ni) trigonal prisms form $M'MO_6$ chains by sharing their triangular faces, and these chains pack in a hexagonal pattern with the alkaline earth elements A (=Ca, Sr, Ba) located at the eight-coordinate sites between the chains (Figure 1). The oxides $Sr_3CuMO_6$ (M = Pt,[8,18] Ir[11]) have a slightly different structure in that each $O_6$ trigonal prism between adjacent $MO_6$ octahedra has the Cu atom near the center of one rectangular face of the prism. The oxides $A_3M'MO_6$ (A = Ca, Sr; M = Rh, Ir; M′ = alkaline earth, Zn, Cd) with unpaired electrons only at the M sites exhibit an antiferromagnetic (AFM) ordering at low temperatures,[3,6,10−12,16] and so do the oxides possessing unpaired electrons only at the M′ sites (e.g., $Sr_3NiPtO_6$ and $Sr_3CuPtO_6$).[8] In the oxides with unpaired electrons at both M′ and M sites (e.g., $Sr_3NiIrO_6$ and $Sr_3CuIrO_6$)[11] and also in $Ca_3Co_2O_6$,[17] ferromagnetic (FM) interactions between spins occur at low temperatures.

For the AFM ordering in the oxides $A_3M'MO_6$ (M = Rh, Ir) with unpaired electrons only at the M sites, direct M···M interactions are not responsible because the nearest-neighbor M···M distances are long. In these oxides, the interchain M···M distances are similar to the intrachain M···M distances, so Battle and co-workers[10,12] emphasized that these oxides are three-dimensional although their structure is commonly described in terms of $M'MO_6$ chains. Vente et al.[10] proposed that the magnetic ordering originates from superexchange interactions involving the M−O···M′···O−M intrachain linkage and the M−O···A···O−M interchain linkage. These pathways are longer than the typical superexchange linkage of M−L−M type,[19] where L refers to a ligand atom. When the valence atomic orbitals of M′ and A lie well outside the energy region of the oxygen 2s/2p orbitals,[20,21] orbital interactions between M′ and O and between A and O become negligible.[22] Then, the

(1) Bergerhoff, G.; Schmitz-Dumont, O. *Z. Anorg. Allg. Chem*. **1956**, *284*, 10.
(2) Randall, J., Jr.; Katz, L. *Acta Crystallogr*. **1959**, *12*, 519.
(3) Sarkozy, R. F.; Moeller, C. W.; Chamberland, B. L. *J. Solid State Chem*. **1974**, *9*, 243.
(4) Ben-Dor, L.; Suss, J. T.; Cohen, S. *J. Cryst. Growth* **1983**, *64*, 395.
(5) Wilkinson, A. P.; Cheetham, A. K. *Acta Crystallogr. C* **1989**, *12*, 519.
(6) Powell, A. V.; Gore, J. G.; Battle, P. D. *J. Alloys Compd*. **1993**, *201*, 73.
(7) Powell, A. V.; Battle, P. D.; Gore, J. G. *Acta Crystallogr. C* **1993**, *49*, 852.
(8) Nguyen, T. N.; Giaquinta, D. M.; zur Loye, H.-C. *Chem. Mater*. **1994**, *6*, 1642.
(9) Frenzen, S.; Müller-Buschbaum, Hk. *Z. Naturforsch. B* **1995**, *50*, 581.
(10) Vente, J. F.; Lear, J. K.; Battle, P. D. *J. Mater. Chem*. **1995**, *5*, 1785.
(11) Nguyen, T. N.; zur Loye, H.-C. *J. Solid State Chem*. **1995**, *117*, 300.
(12) Segal, N.; Vente, J. F.; Bush, T. S.; Battle, P. D. *J. Mater. Chem*. **1996**, *6*, 395.
(13) Lampe-Önnerud, C.; zur Loye, H.-C. *Inorg. Chem*. **1996**, *35*, 2155.
(14) Claridge, J. B.; Layland, R. C.; Adams, R. D.; zur Loye, H.-C. *Z. Anorg. Allg. Chem*. **1997**, *623*, 1131.
(15) Nunez, P.; Rzeznik, M.; zur Loye, H.-C. *Z. Anorg. Allg. Chem*. **1997**, *623*, 1269.
(16) Nunez, P.; Trail, S.; zur Loye, H.-C. *J. Solid State Chem*. **1997**, *130*, 35.
(17) Aasland, S.; Fjellvag, H.; Hauback, B. *Solid State Commun*. **1997**, *101*, 187.
(18) Wilkinson, A. P.; Cheetham, A. K.; Kunnman, W.; Kvick, A. *Eur. J. Solid State Inorg. Chem*. **1991**, *28*, 453.
(19) Kahn, O. *Molecular Magnetism:* VCH Publishers: Weinheim, 1993.
(20) Clementi, E.; Roetti, C. *At. Data Nucl. Data Tables* **1974**, *14*, 177.
(21) McLean, A. D.; McLean, R. S. *At. Data Nucl. Data Tables* **1981**, *26*, 197.

10.1021/ic9813819 CCC: $18.00 
Published on Web 04/14/1999

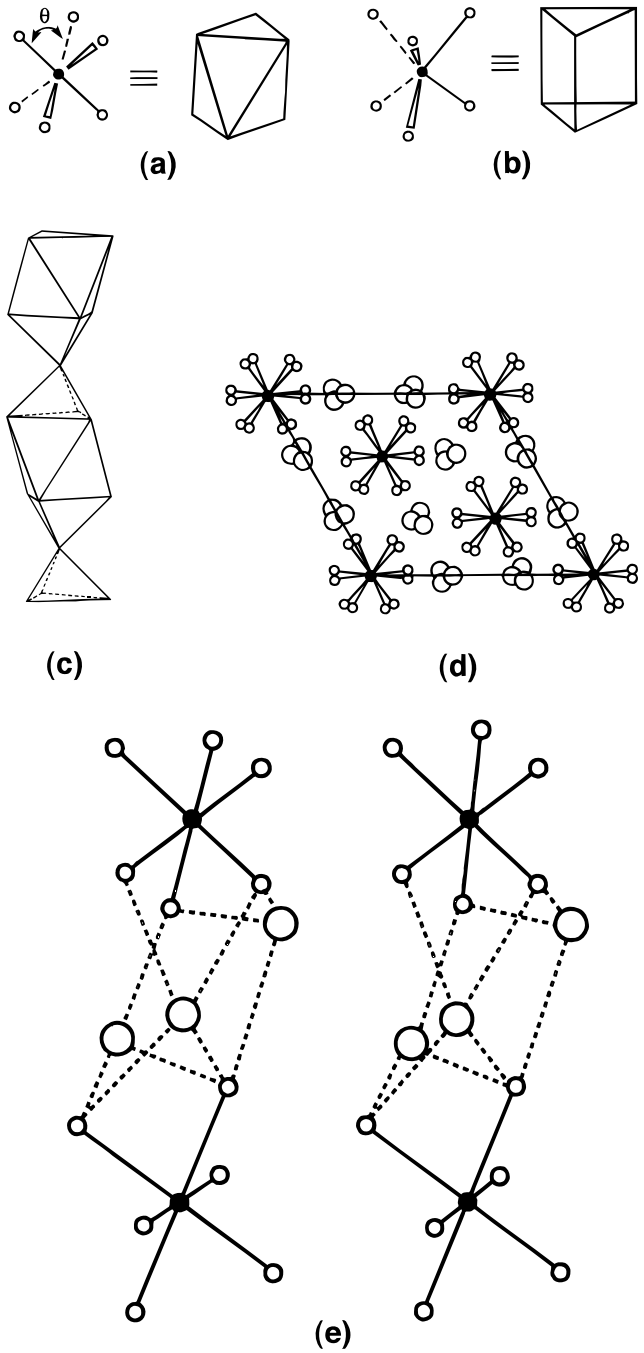


**Figure 1.** Building blocks of the oxide $A_3M'MO_6$ of the $K_4CdCl_6$ structure type: (a) $MO_6$ octahedron. (b) $M'O_6$ trigonal prism. (c) $M'MO_6$ chain, where each trigonal prism is slightly twisted as can be seen from Figure 1d. (d) Packing of the $M'MO_6$ chains in $A_3M'MO_6$, where the alkaline earth atoms A are represented by the large open circles. (e) Stereoview of two adjacent $MO_6$ octahedra between the nearest-neighbor $M'MO_6$ chains, with three A atoms connecting the two. The A···O contacts shorter than 2.5 Å are shown by dashed lines.

superexchange interactions through the M−O···M′···O−M and M−O···A···O−M pathways may not be significant. To resolve this question, it is necessary to examine the nature of the superexchange interaction in these oxides.

The occurrence of a long-range magnetic order (i.e., the AFM ordering) in the oxides $A_3M'MO_6$ (M = Rh, Ir) suggests that the spin−spin interactions between the M sites cannot be one-dimensional. The onset temperature of an AFM ordering (i.e., the Néel temperature $T_N$) is high when adjacent spins have a strong antiferromagnetic interaction. From the observation that the Néel temperature of $Sr_3CaRhO_6$ ($T_N$ = 7 K) is the same as that of $Sr_4RhO_6$ despite a marked decrease in the Rh···Rh distance along the chain, Vente et al.[10] suggested that the interchain spin−spin interactions are important in causing the onset of long-range magnetic order. $Sr_3ZnIrO_6$ and $Sr_3CdIrO_6$ have considerably higher Néel temperatures (i.e., 19 and 22 K, respectively) than do the oxides with M′ = alkaline earth elements. This led Segal et al.[12] to suggest that the $d^{10}$ cores of the $Zn^{2+}$ and $Cd^{2+}$ cations are important. So far these suggestions have not been tested by electronic structure studies. The only report on the electronic structures of $A_3M'MO_6$ is Vajenine et al.'s work.[23] Their electronic band structure calculations for the $M'MO_6$ chains of $Sr_3M'MO_6$ (M′ = Co, Ni; M = Pt, Ir) showed that both direct and oxygen-mediated intrachain M′···M interactions are very small (for further discussion, see below).

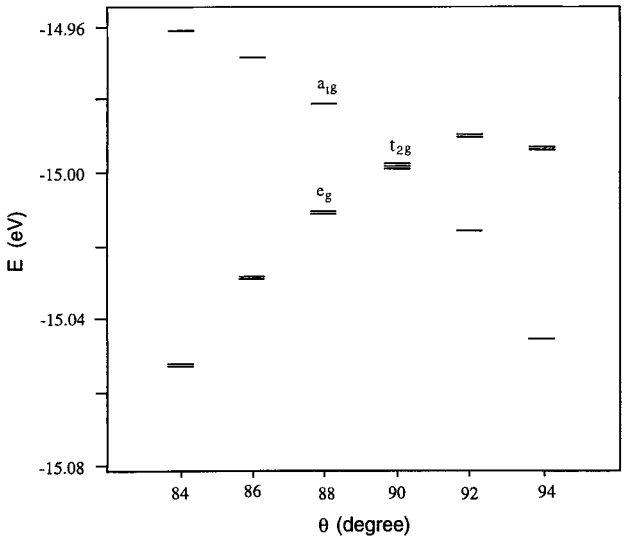


**Figure 2.** Split of the $t_{2g}$-block levels of an $MO_6$ octahedron as a function of the O−M−O bond angle $\theta$ calculated by using an $(RhO_6)^{8-}$ anion with Rh−O = 2.026 Å.

In the present work we examine the antiferromagnetic ordering phenomenon in the oxides $A_3M'RhO_6$ and $A_3M'IrO_6$ (M′ = alkaline earth, Zn, Cd, Na), whose spin-carrying units are their octahedral $(MO_6)^{(6+n)-}$ (M = Rh, Ir; $n$ = 1, 2) anions. Intrachain and interchain spin−spin interactions between these anions were examined by performing extended Hückel[24,25] molecular orbital calculations. The short intrachain and interchain contact distances between adjacent anions were also analyzed to see how the intrachain and interchain interactions depend on the nature of the $A^{2+}$ and $M'^{n+}$ cations. Our study of the oxides $A_3M'MO_6$ in which both M′ and M are transition metal atoms will be reported elsewhere.[26]

## 2. Dimer Model for Spin−Spin Interactions

When the O−M−O bond angle $\theta$ (see Figure 1a) deviates from 90°, the $t_{2g}$-block levels of an octahedral $(MO_6)^{(6+n)-}$ anion split into $a_{1g}$ and $e_g$ levels as shown in Figure 2. (The values of

(22) Albright, T. A.; Burdett, J. K.; Whangbo, M.-H. *Orbital Interaction in Chemistry*; Wiley: New York, 1985; Chapter 2.

(23) Vajenine, G. V.; Hoffmann, R.; zur Loye, H.-C. *Chem. Phys.* **1996**, *204*, 469.

(24) Hoffmann, R. *J. Chem. Phys.* **1963**, *39*, 1397.

(25) Our calculations were carried out by employing the CAESAR program package (Ren, J.; Liang, W.; Whangbo, M.-H. *Crystal and Electronic Structure Analysis Using CAESAR*; 1998. For details, see: http://www.PrimeC.com/.).

(26) Lee, K.-S.; Koo, H.-J.; Whangbo, M.-H. In preparation.

**Table 1.** Exponents $\zeta_i$ and Valence Shell Ionization Potentials $H_{ii}$ of Slater-Type Orbitals $\chi_i$ Used for Extended Hückel Tight-Binding Calculation[a]

| atom | $\chi_i$ | $H_{ii}$ (eV) | $\zeta_i$ | $c_1$[b] | $\zeta_i'$ | $c_2$[b] |
|---|---|---|---|---|---|---|
| Rh | 5s | −6.62 | 2.089 | 1.0 | | |
| Rh | 5p | −3.52 | 1.450 | 1.0 | | |
| Rh | 4d | −16.4 | 4.561 | 0.5576 | 2.365 | 0.5919 |
| Ir | 6s | −6.59 | 2.457 | 1.0 | | |
| Ir | 6p | −3.33 | 1.810 | 1.0 | | |
| Ir | 5d | −15.2 | 4.680 | 0.6195 | 2.490 | 0.5384 |
| O | 2s | −33.7 | 2.688 | 0.7076 | 1.675 | 0.3745 |
| O | 2p | −17.1 | 3.694 | 0.3322 | 1.659 | 0.7448 |
| Mg | 3s | −9.00 | 1.472 | 0.4724 | 0.892 | 0.6101 |
| Mg | 3p | −6.60 | 1.060 | 1.0 | | |
| Ca | 4s | −5.31 | 1.434 | 0.5179 | 0.867 | 0.5836 |
| Ca | 4p | −3.79 | 1.060 | 1.0 | | |
| Sr | 5s | −4.84 | 1.630 | 0.5087 | 0.961 | 0.6091 |
| Sr | 5p | −3.47 | 1.170 | 1.0 | | |
| Zn | 4s | −7.61 | 2.221 | 0.4843 | 1.195 | 0.6304 |
| Zn | 4p | −4.23 | 1.540 | 1.0 | | |
| Zn | 3d | −19.6 | 7.349 | 0.4431 | 3.139 | 0.6971 |
| Cd | 5s | −7.07 | 2.352 | 0.5805 | 1.292 | 0.5820 |
| Cd | 5p | −4.26 | 1.670 | 1.0 | | |
| Cd | 4d | −18.0 | 5.213 | 0.5853 | 2.706 | 0.5720 |

[a] $H_{ii}$'s are the diagonal matrix elements $\langle\chi_i|H^{\text{eff}}|\chi_i\rangle$, where $H^{\text{eff}}$ is the effective Hamiltonian. In our calculations of the off-diagonal matrix elements $H^{\text{eff}} = \langle\chi_i|H^{\text{eff}}|\chi_j\rangle$, the weighted formula was used. See: Ammeter, J.; Bürgi, H.-B.; Thibeault, J.; Hoffmann, R. *J. Am. Chem. Soc*. **1978**, *100*, 3686. [b] Contraction coefficients used in the double-$\zeta$ Slater-type orbital.

**Table 2.** Values of the Intrachain and Interchain $\Delta E_a$ and $\Delta E_e$ (in meV) Calculated for Various Oxides $A_3M'Mo_6$[a]

| | intrachain | | interchain | | |
|---|---|---|---|---|---|
| $A_3M'MO_6$ | $\Delta E_a$ | $\Delta E_e$ | $\Delta E_a$ | $\Delta E_e$(L) | $T_N$ (K) |
| $Sr_3MgRhO_6$ | 127 (115) | 79 (49) | 17 (16) | 52 (45) | ∼13 (ref 16) |
| $Sr_3CaRhO_6$ | 70 (64) | 42 (25) | 27 (23) | 43 (43) | 7 (ref 10) |
| $Sr_4RhO_6$ | 48 (44) | 29 (16) | 10 (4) | 80 (73) | 7 (ref 10) |
| $Sr_3MgIrO_6$ | 103 (85) | 61 (36) | 10 (12) | 48 (38) | ∼13 (ref 16) |
| $Sr_3CaIrO_6$ | 58 (49) | 38 (20) | 14 (13) | 43 (39) | 14 (ref 12) |
| $Sr_4IrO_6$ | 36 (29) | 26 (12) | 10 (2) | 64 (56) | 12 (ref 6) |
| $Ca_4IrO_6$ | 64 (54) | 44 (22) | 12 (8) | 104 (80) | 16 (ref 12) |
| $Sr_3ZnIrO_6$[b] | 94 (81) | 69 (34) | 12 (13) | 48 (39) | 19 (ref 12) |
| $Sr_3CdIrO_6$[c] | 33 (52) | 84 (21) | 12 (15) | 50 (41) | 22 (ref 12) |
| $Ca_3NaIrO_6$ | 39 (21) | 59 (49) | 12 (9) | 100 (89) | *d* |
| $Ca_3NaRuO_6$ | 57 (48) | 37 (20) | 15 (5) | 96 (83) | *d* |
| $Sr_3NaRuO_6$ | 48 (39) | 32 (15) | 8 (3) | 69 (58) | *d* |

[a] The values calculated for the dimers with the $A^{2+}$ and $M'^{n+}$ cations are presented without parentheses, and those without the cations are presented in parentheses. [b] The intrachain $\Delta E_a$ and $\Delta E_e$ values calculated without using the 3d orbitals of Zn are 101 and 62 meV, respectively. [c] The intrachain $\Delta E_a$ and $\Delta E_e$ values calculated without using the 4d orbitals of Cd are 71 and 49 meV, respectively. [d] Unknown.

$\theta$ found for various $MO_6$ octahedral units are listed in Table 3.) The oxides $A_3M'MO_6$ (M = Rh, Ir) with diamagnetic $M'^{2+}$ cations have isolated $(MO_6)^{8-}$ octahedral anions. Each $(MO_6)^{8-}$ (M = Rh, Ir) anion has one unpaired electron in the $a_{1g}/e_g$ levels because its $M^{4+}$ cation has a $d^5$ electron count. Each $(IrO_6)^{7-}$ anion of $Ca_3NaIrO_6$ has an $Ir^{5+}$ ($d^4$) cation and hence two unpaired electrons in the $a_{1g}/e_g$ levels. Each $(RuO_6)^{7-}$ anion of $A_3NaRuO_6$ (A = Ca, Sr) has three unpaired electrons in the $a_{1g}/e_g$ levels due to the $d^3$ electron count for its $Ru^{5+}$ cation. Adjacent $(MO_6)^{(6+n)-}$ anions are connected by one $M'^{n+}$ ($n$ = 1 or 2) cation within each $M'MO_6$ chain (Figure 1c) and by three $A^{2+}$ cations between the nearest-neighbor $M'MO_6$ chains (Figure 1e).

In general, the strength of a spin−spin interaction between adjacent spin centers is described by the exchange coupling constant, $J$. The latter is written as the sum of the ferromagnetic term $J_F$ (>0) and the antiferromagnetic term $J_{AF}$ (<0).[19,27] For antiferromagnetic systems, the $J_{AF}$ term dominates over the $J_F$ term. From the viewpoint of molecular orbital calculations for a spin dimer (i.e., two adjacent spin-carrying monomers),[28] the strength of spin−spin interaction (i.e., the magnitude of $J_{AF}$) is proportional to the square of the energy difference $\Delta E$ between the highest two singly filled levels of the spin dimer, i.e., $|J_{AF}| \propto (\Delta E)^2$ (Figure 3). Recently, this approach has been found useful in understanding the spin−spin exchange interactions of the layered oxides $Cs_2V_4O_9$, $CaV_4O_9$, and $[H_2N(CH_2)_4NH_2]$-$V_4O_9$[29] as well as the layered oxides $\alpha'$-$NaV_2O_5$, $CaV_2O_5$, and $MgV_2O_5$.[30]

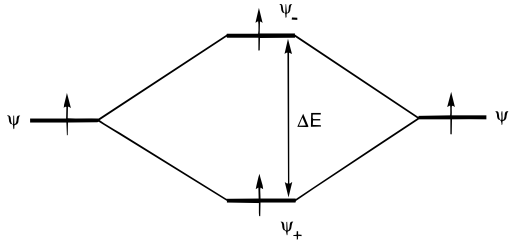


**Figure 3.** Interaction between the spin-containing orbitals $\psi$ of two adjacent spin monomers leading to the two singly filled levels ($\psi_+$ and $\psi_-$) of the spin dimer, which are represented by linear combinations of two orbitals $\psi$. The electron configuration shown in this figure is one of the four in which the $\psi_+$ and $\psi_-$ levels are each singly occupied (ref 28). The square of the energy gap, $(\Delta E)^2$, is proportional to the antiferromagnetic spin exchange parameter $J_{AF}$ between the two adjacent spins.

**Table 3.** Shortest O···O Contact Distances between Adjacent $MO_6$ Octahedra, O−M−O Bond Angles $\theta$ of $MO_6$ Octahedra, and Cation Radius Ratio in $A_3M'Mo_6$

| | O···O distance (Å) | | | | |
|---|---|---|---|---|---|
| $A_3M'MO_6$ | intrachain | interchain | $\theta$(deg) | $R$ | ref |
| $Sr_3MgRhO_6$ | 3.009 | 3.155 | 84.86 | 0.57 | 16 |
| $Sr_3CaRhO_6$ | 3.341 | 3.062 | 87.99 | 0.79 | 10 |
| $Sr_4RhO_6$ | 3.534 | 2.999 | 89.13 | 0.94 | 10 |
| $Sr_3MgIrO_6$ | 3.076 | 3.121 | 85.68 | 0.57 | 16 |
| $Sr_3CaIrO_6$ | 3.370 | 3.055 | 88.27 | 0.79 | 12 |
| $Sr_4IrO_6$ | 3.622 | 2.992 | 90.29 | 0.94 | 6 |
| $Ca_4IrO_6$ | 3.351 | 2.870 | 89.98 | 0.89 | 3, 12 |
| $Sr_3ZnIrO_6$ | 3.104 | 3.094 | 85.06 | 0.59 | 12 |
| $Sr_3CdIrO_6$ | 3.335 | 3.026 | 86.25 | 0.75 | 12 |
| $Ca_3NaIrO_6$ | 3.409 | 2.841 | 91.09 | 0.91 | 14 |
| $Ca_3NaRuO_6$ | 3.398 | 2.837 | 90.76 | 0.91 | 14 |
| $Sr_3NaRuO_6$ | 3.498 | 2.995 | 90.01 | 0.81 | 9 |

Consequently, to estimate how strongly the spins at adjacent M sites interact, it is necessary to calculate how strongly the $a_{1g}/e_g$ levels of one $(MO_6)^{(6+n)-}$ anion interact with those of its adjacent $(MO_6)^{(6+n)-}$ anion via the $A^{2+}$ and $M'^{n+}$ cations. Since each $(MO_6)^{(6+n)-}$ anion carries a spin, we perform molecular orbital calculations for the intrachain dimer $[(MO_6)^{(6+n)-}(M'^{n+})$-$(MO_6)^{(6+n)-}]$ and the interchain dimer $[(MO_6)^{(6+n)-}(A^{2+})_3$-$(MO_6)^{(6+n)-}]$.

The split of the $t_{2g}$-block level into the $a_{1g}$ and $e_g$ levels (Figure 2) in a slightly distorted $(MO_6)^{(6+n)-}$ anion is very small. Therefore, the $a_{1g}$ level and each of the doubly degenerate $e_g$ levels should have an equal probability of having an unpaired spin even for the $d^5$ and $d^4$ electron counts (from the viewpoint

(27) Anderson, P. W. *Phys. Rev.* **1959**, *115*, 2.
(28) Hay, P. J.; Thibeault, J. C.; Hoffmann, R. *J. Am. Chem. Soc*. **1975**, *97*, 4884.
(29) Zhang, Y.; Warren, C. J.; Haushalter, R. C.; Clearfield, A.; Seo, D.-K.; Whangbo, M.-H. *Chem. Mater*. **1998**, *10*, 1059.
(30) Koo, H.-J.; Whangbo, M.-H. *Solid State Commun*., in press.

of the multiconfiguration ground state). The $a_{1g}$ levels of two adjacent $(MO_6)^{(6+n)-}$ anions interact to form the two levels (say, $a_+$ and $a_-$) of the dimer that are represented by linear combinations of the two $a_{1g}$ levels. A large energy gap $\Delta E_a$ between the $a_+$ and $a_-$ levels leads to a strong AFM interaction when each $a_{1g}$ level contains a spin. Likewise, the $e_g$ levels of two adjacent $(MO_6)^{(6+n)-}$ anions interact to form the two levels (say, $e_+$ and $e_-$) of the dimer that are represented by linear combinations of the two $e_g$ levels. A large energy gap $\Delta E_e$ between the $e_+$ and $e_-$ levels leads to a strong AFM interaction when each $e_g$ level contains a spin.

The intrachain dimer $[(MO_6)^{(6+n)-}(M'^{n+})(MO_6)^{(6+n)-}]$ keeps the threefold rotational symmetry along the chain direction, so that the degeneracy of the $e_g$ level is not split by the intrachain interaction. However, this is not the case for the interchain dimer $[(MO_6)^{(6+n)-}(A^{2+})_3(MO_6)^{(6+n)-}]$, and the degeneracy of the $e_g$ level is split by the interchain interaction. Therefore, two different $\Delta E_e$ values result from the interchain interaction involving the $e_g$ levels. The larger and smaller interchain $\Delta E_e$ values may be denoted by $\Delta E_e(L)$ and $\Delta E_e(S)$, respectively.

To assess the importance of the $M'^{n+}$ and $A^{2+}$ cations in determining the magnitudes of the intrachain and interchain interactions, we also calculate the $\Delta E_a$ and $\Delta E_e$ values using the intrachain and interchain dimers without the intervening $M'^{n+}$ and $A^{2+}$ cations. To examine the role of the $d^{10}$ cores of the $Zn^{2+}$ and $Cd^{2+}$ cations in determining the magnitudes of the intrachain interactions, we calculate the intrachain $\Delta E_a$ values using the intrachain dimers with and without the 3d and 4d orbitals $Zn^{2+}$ and $Cd^{2+}$, respectively.

### 3. Calculations

The parameters of the atomic orbitals used in our molecular electronic structure calculations are summarized in Table 1. Double-$\zeta$ Slater-type orbitals (STOs) [20,21] were used not only for the *n*d orbitals of the transition metal M but also for the 2s/2p orbitals of oxygen and the *n*s orbitals of A and M′. Our calculations using single-$\zeta$ STOs for the 2s/2p orbitals of oxygen lead to very small $\Delta E_a$ and $\Delta E_e$ values, which are too small to be meaningful in discussing the spin−spin interactions of $A_3M'MO_6$. Vajenine et al.'s finding[23] that both direct and oxygen-mediated intrachain M′···M interactions in $Sr_3M'MO_6$ (M′ = Co, Ni; M = Pt, Ir) are very small originates from their use of single-$\zeta$ STOs for the 2s/2p orbitals of oxygen.

From the electronic structure studies of conducting salts of organic donor molecules, it is well-known[31,32] that overlap integrals between organic donor molecules are strongly enhanced when double-$\zeta$ STOs are used. The diffuse components of such orbitals provide diffuse tails that are essential for intermolecular overlap in molecular crystals. The oxides $A_3M'MO_6$ (M = Rh, Ir) consist of isolated $(MO_6)^{(6+n)-}$ ions, and a moderate overlap between them is needed to explain their magnetic interactions. This requires that the 2s/2p atomic orbitals of oxygen have diffuse tails, which are provided by the double-$\zeta$ STOs. Similarly, the *n*s orbitals of A and M′ were also represented by double-$\zeta$ STOs to better describe the orbital overlap in the A···O and M′···O linkages.

### 4. Trends in the Spin−Spin Interactions

The $\Delta E_a$ and $\Delta E_e$ values calculated for the oxides $A_3M'MO_6$ (M = Rh, Ir) with diamagnetic $M'^{n+}$ cations are listed in Table 2. Our calculations for the interchain dimers show that the $\Delta E_e$(S) values are close to 0 and hence are not listed in Table 2. The $\Delta E_a$ and $\Delta E_e$ values calculated using the dimers with the intervening $M'^{n+}$ and $A^{2+}$ cations are presented without parentheses, and those calculated without these cations are given in parentheses. Also listed in Table 2 are the available Néel temperatures of the oxides $A_3M'MO_6$.

There are several important observations to make from Table 2: (a) For the intrachain interactions of $Sr_3M'RhO_6$ and $Sr_3M'IrO_6$ (M′ = Mg, Ca, Sr), $\Delta E_a$ and $\Delta E_e$ decrease with increasing the size of M′, and $\Delta E_a$ is larger than $\Delta E_e$ for each M′. (b) For the interchain interactions of $Sr_3M'RhO_6$ and $Sr_3M'IrO_6$ (M′ = Mg, Ca, Sr), $\Delta E_a$ is smaller than $\Delta E_e$(L) for each M′, and the largest $\Delta E_e$(L) is found for M′ = Sr. (c) When A = Sr and M′ = Mg or Zn, the intrachain $\Delta E_a$ is substantially larger than the interchain $\Delta E_e$(L), i.e., the intrachain interaction is substantially stronger than the interchain interaction. (d) When M′ and A are identical, the interchain $\Delta E_e$(L) is significantly larger than the intrachain $\Delta E_a$, i.e., the interchain interaction is significantly stronger than the intrachain interaction. This is also the case when A = Ca and M′ = Na.

To understand how the $A^{2+}$ and $M'^{n+}$ cations affect the intrachain and interchain interactions, we first observe that the $\Delta E_a$ and $\Delta E_e$ values calculated using the dimers with the intervening $M'^{n+}$ and $A^{2+}$ cations are comparable in magnitude to those calculated without using them, except for the intrachain $\Delta E_e$ values that are enhanced substantially by the $M'^{n+}$ cations. In most cases, the $M'^{n+}$ and $A^{2+}$ cations contribute only slightly to the interactions between the $t_{2g}$-block orbitals of adjacent $(MO_6)^{(6+n)-}$ anions. This means that the superexchange interactions in the oxides $A_3M'MO_6$ occur mainly through the short intrachain and interchain M−O···O−M linkages between adjacent $(MO_6)^{(6+n)-}$ anions, and that the short intrachain and interchain O···O contacts between adjacent $(MO_6)^{(6+n)-}$ anions are crucial for the spin−spin interactions in the oxides $A_3M'MO_6$. Therefore, it is necessary to analyze how the short intrachain and interchain O···O distances vary as a function of the size of the $A^{2+}$ and $M'^{n+}$ cations.

For simplicity, Table 3 lists only the shortest intrachain and interchain O···O contact distances between adjacent $(MO_6)^{(6+n)-}$ anions. Also listed in Table 3 are the O−M−O bond angles $\theta$ of the $(MO_6)^{(6+n)-}$ anions (Figure 1a). These geometrical parameters were obtained from the reported crystal structures of $A_3M'MO_6$. To understand the trends in the O···O contact distances and the O−M−O bond angles, one needs to consider the six-coordinate ionic radii of the $M'^{n+}$ cations (i.e., 0.72 Å for $Mg^{2+}$, 1.00 Å for $Ca^{2+}$, 1.18 Å for $Sr^{2+}$, 0.74 Å for $Zn^{2+}$, 0.95 Å for $Cd^{2+}$, and 1.02 Å for $Na^+$)[33] and the eight-coordinate ionic radii of the $A^{2+}$ cations (i.e., 1.12 Å for $Ca^{2+}$ and 1.26 Å for $Sr^{2+}$).[33] Table 3 lists the ratio $R$ of the $M'^{n+}$ cation radius to the $A^{2+}$ cation radius for each oxide.

Table 3 reveals that the O−M−O bond angle $\theta$ is close to 90° when M′ and A are identical. For M′ = Na, the bond angle is close to 90° for A = Sr and larger than 90° for A = Ca. When a divalent M′ is smaller than A, the bond angle is smaller than 90°. With increasing the size of $M'^{n+}$ for a given $A^{2+}$, the intrachain O···O distance increases hence decreasing the intrachain interaction, but the interchain O···O distance decreases thus increasing the interchain interaction. When the $M'^{n+}$ cation is very small compared with the $A^{2+}$ cation (i.e., $R < 0.6$), the intrachain O···O contact is either shorter than, or nearly equal to, the interchain O···O contact, and the intrachain interaction

(31) Whangbo, M.-H.; Williams, J. M.; Leung, P. C. W.; Beno, M. A.; Emge, T. J.; Wang, H. H.; Carlson, K. D.; Crabtree, G. W. *J. Am. Chem. Soc.* **1985**, *107*, 5815.

(32) Williams, J. M.; Wang, H. H.; Emge, T. J.; Geiser, U.; Beno, M. A.; Leung, P. C. W.; Carlson, K. D.; Thorn, R. J.; Schultz, A. J.; Whangbo, M.-H. *Prog. Inorg. Chem.* **1987**, *35*, 51.

(33) Shannon, R. D. *Acta Crystallogr. A* **1976**, *32*, 751.

is significantly larger than the interchain interaction. An increase in the radius ratio $R$ increases the intrachain O···O contact distance while decreasing the interchain O···O contact distance. This weakens the intrachain interaction but enhances the interchain interaction. When the sizes of the $M'^{n+}$ and $A^{2+}$ cations are similar, the interchain interaction becomes considerably stronger than the intrachain interaction. Thus, the effects of the $A^{2+}$ and $M'^{n+}$ cations on the intrachain and interchain interactions are primarily related to how the intrachain and interchain O···O contacts between adjacent $(MO_6)^{(6+n)-}$ anions depend on the sizes of these cations.

## 5. Discussion

For all of the oxides listed in Table 2, neither the intrachain nor the interchain interactions dominate. Even for those in which one interaction is significantly stronger than the other interaction, the weaker interaction is not negligible. This supports the conclusion of Battle and co-workers[10,12] that these oxides are three-dimensional.

Let us consider the similarity in the Néel temperatures of $Sr_3CaMO_6$ and $Sr_4MO_6$ (M = Rh, Ir). Table 2 shows that the intrachain interaction is stronger than the interchain interaction in $Sr_3CaMO_6$, while the opposite is the case in $Sr_4MO_6$. Nevertheless, the intrachain $\Delta E_a$ of $Sr_3CaMO_6$ is comparable in magnitude to the interchain $\Delta E_e$(L) of $Sr_4MO_6$. This accounts for why the Néel temperatures of $Sr_3CaMO_6$ and $Sr_4MO_6$ are the same,[6,10,12] despite a large difference in the M···M distances along the chain.[6,10,12]

We now examine the similarity in the Néel temperatures of $Sr_3ZnIrO_6$ and $Sr_3CdIrO_6$. Table 2 shows that for both compounds the intrachain interaction is stronger than the interchain interaction. Our calculations of the intrachain $\Delta E_a$ and $\Delta E_e$ values with and without the Zn 3d and Cd 4d orbitals reveal that the effect of the Cd 4d orbitals is stronger than that of the Zn 3d orbitals (see the footnotes *b* and *c* of Table 2). This is understandable because the Cd 4d orbitals are more diffuse than the Zn 3d orbitals, i.e., the $d^{10}$ core of $Cd^{2+}$ is more polarizable than that of $Zn^{2+}$. Note that the Cd 4d orbitals reduce the intrachain $\Delta E_a$ but increase the intrachain $\Delta E_e$. The intrachain $\Delta E_a$ is larger than the intrachain $\Delta E_e$ in $Sr_3ZnIrO_6$, but the opposite is the case in $Sr_3CdIrO_6$. Nevertheless, the intrachain $\Delta E_a$ of $Sr_3ZnIrO_6$ is similar in magnitude to the intrachain $\Delta E_e$ of $Sr_3CdIrO_6$. This explains why the Néel temperature of $Sr_3CdIrO_6$ is comparable to that of $Sr_3ZnIrO_6$,[12] despite a significant increase in the Ir···Ir distance along the chain. This is in support of Segal et al.'s suggestion[12] that a polarizable $d^{10}$ core is important in determining the Néel temperature and, thus, Vente et al.'s suggestion[10] of the M−O···$M'^{n+}$···O−M superexchange pathway. This means that the 4d orbitals of the $Cd^{2+}$ cation are diffuse enough to overlap with the oxygen 2p orbitals.

The Néel temperatures of $Sr_3CaRhO_6$ and $Sr_4RhO_6$ are smaller than those of the Ir analogues,[6,10,12] which led Vente et al.[10] to suggest that the greater degree of covalency in the 5d $Ir^{4+}$ system is an important factor. If $Sr_3CaRhO_6$ and $Sr_4RhO_6$ have a smaller intrachain $\Delta E_a$ and a smaller interchain $\Delta E_e$(L) value than do the Ir analogues, respectively, then the difference between the Rh and Ir analogues can be explained. However, the opposite is found in Table 2. The $t_{2g}$-block levels of an $(MO_6)^{(6+n)-}$ anion have small coefficients on the oxygen atoms. Thus the overlap between the $t_{2g}$-block levels of adjacent $(MO_6)^{(6+n)-}$ anions, which occurs via the short O···O contacts between the anions, is very small. The difference between the Rh−O···O−Rh and Ir−O···O−Ir linkages, being caused by a change away from the O···O contact, may be too small to correctly reproduce by extended Hückel electronic structure calculations.

## 6. Concluding Remarks

In the oxides $A_3M'MO_6$ containing spins only at the M sites, neither the intrachain nor the interchain spin−spin interactions dominate, and the superexchange interactions occur mainly through the intrachain and interchain M−O···O−M linkages. These observations result from the fact that the $t_{2g}$-block orbitals of adjacent $(MO_6)^{(6+n)-}$ anions interact primarily through their short O···O contacts. An exceptional case is the Ir−O···$Cd^{2+}$···O−Ir linkage of $Sr_3CdIrO_6$, for which the intrachain $\Delta E_e$ is enhanced by the 4d orbitals of $Cd^{2+}$. The intrachain interaction is substantially stronger than the interchain interaction when the $M^{n+}$ cation is very small compared with the $A^{2+}$ cation. The opposite is found when the size of the $M^{n+}$ cation becomes close to that of the $A^{2+}$ cation.

**Acknowledgment.** The work at North Carolina State University was supported by the Office of Basic Energy Sciences, Division of Materials Sciences, U.S. Department of Energy, under Grant DE-FG05-86ER45259. K.-S.L. thanks the Korean Research Foundation for the financial support during 1997.

IC9813819